# Acoustic Characterization of a Shallow Water Site

P. Cable, W. Marshall

*BBN Systems and Technologies, New London, CT 06320,USA*

T. Kooij, G. Skarda, K. Waldman

*BBN Systems and Technologies, Arlington, VA 22209, USA*

**Abstract** Results are presented from an exercise aimed at providing a low frequency active sonar environmental characterization of a specific shallow water site in the Gulf of Mexico. Downward refracting acoustic transmission and reverberation measurements were made in 100 fathom water from 25 Hz to 1 kHz using explosive sources detonated at mid-water depth. The receiving sensors were two 25 element, nested aperture hydrophone line arrays, one vertical near the bottom and the other horizontal on the bottom. Transmission data have been analyzed to yield transmission loss, multipath induced time spread and transverse spatial coherence. From the reverberation data bottom scattering strengths and horizontal reverberation directionality have been determined. The data presented will permit direct estimates of reverberation limited active sonar performance to be made for this environment.

## 1. Introduction

Through the cumulative effects of boundary interactions, detection performance of search and surveillance sonars is more severely influenced by the acoustic environment in shallow water than in deep water. Excepting performance in surface ducted environments, active sonar transmissions in shallow water quite typically are dominated acoustically by multiple bottom encounters that result in high transmission loss and substantial reverberation from bottom backscatter.

Unfortunately, quantitative determinations of achievable sonar performance in shallow water are complicated by the degree of variability both within and among geographic areas. It is therefore of importance to sonar design and performance prediction to have environmental characterizations that comprehend the key acoustic parameters for each area of interest. Area Characterization Test I (ACT I), conducted in the Gulf of Mexico in September 1992 at the edge of the continental shelf, had, as one primary objective, a complete sonar environment characterization of the exercise site. Completeness here refers to a sufficiently detailed environmental description to support modeling of sonar performance for design and evaluation and to facilitate extrapolation of results to other sites.

For shallow water active sonar performance the dominant factor is the reverberation from a bottom patch in the vicinity of the target and it is a reasonable approximation to assume that transmission loss to the bottom patch is the same as that to the target. The target echo will be larger than the reverberation if the strength of the target exceeds the effective target strength of the bottom patch (specified by active area and scattering strength) and detection of the target is possible if the difference is larger than the detection threshold. The contributing area of the reverberant bottom patch is determined by the horizontal receive

array beamwidth, the target echo length (determined by transmit pulse resolution, target length and temporal dispersion of the environment) and by the target-to-receiver range. Thus, for a given target strength, the key environmental parameters that establish the maximum detection range from the receiver are bottom scattering strength, propagation induced pulse spreading, and validity of the two underlying assumptions concerning perfect spatial coherence of the target echo and equal transmission loss for target and reverberation. In addition, it is necessary that the energy source level be large enough to produce a target echo above ambient noise.

In this paper initial results of ACT I will be reviewed and discussed in the context of characterizing the environment in the spirit of the sonar equation as described above. More detailed analyses of the data and evaluations necessary to extrapolate understanding to other areas will be taken up in future reports.

## 2. Test Description

ACT I was conducted from September 18-29, 1992 in a 120 km X 120 km area of the Gulf of Mexico on the northern end of the West Florida Shelf. The test site and bathymetry are shown in Figure 1, which illustrates a gentle upslope of 2.5 m/km to the northeast of the site center and a downslope of 5 m/km to the southwest of the site center. A schematic of the experimental setup is shown in Figure 2. Signals and reverberation in the band 25 Hz to 1 kHz from explosive sources (1.72 kg of Comp B explosive) dropped from the source ship and detonated at 90 m depth were received on two collocated 25 element hydrophone line arrays, one vertical near the bottom and the other deployed horizontally on the bottom. The orientation of the horizontal line array was along the direction of the bathymetry gradient to establish observation symmetry for the reciprocal beams formed with the horizontal line array.

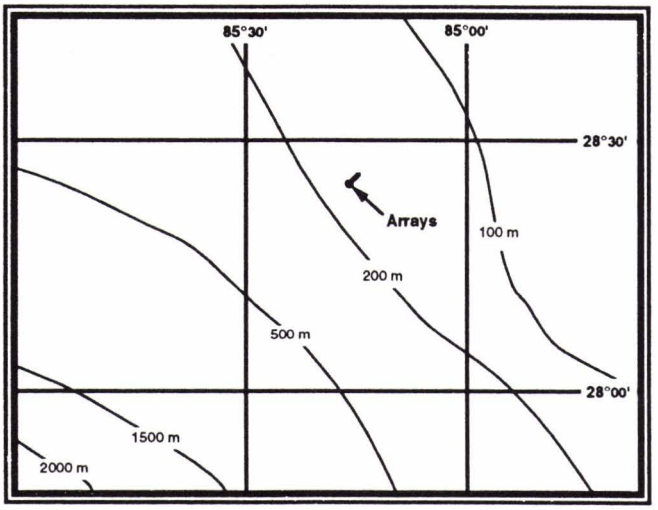


Figure 1. ACT I site and bathymetry with the location of the bottomed receive arrays indicated.

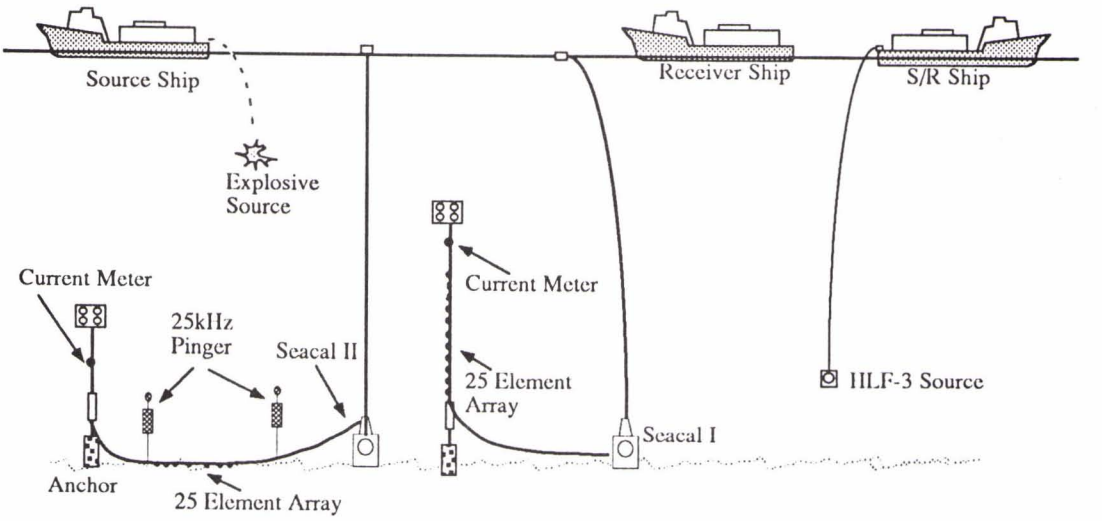


Figure 2. Schematic representation of ACT I experimental setup.

Each array was configured as three nested subapertures with half wavelength element spacings at 100, 200 and 400 Hz and each array was connected electrically to one of two Seacal oceanographic data collection systems[1]. One feature of the arrays was the use of dual sensitivity hydrophones which could be reconfigured through the Seacal units to provide the necessary dynamic range interval to capture either transmission or reverberation data. The Seacal units were periodically retrieved, the acoustic data removed and the units refurbished and redeployed by the receiver monitoring ship. The recovered data were processed onboard the monitoring ship to obtain initial results for guiding test conduct and insuring data quality.

For determination of bottom scattering strength using a calibrated echo, a computer controlled signal repeater was suspended near the bottom from a third ship. Positioning of the ships was determined by differential Global Positioning System (GPS) to within an accuracy of ±2 m and the location of the receiving arrays was determined to the same accuracy by means of a 25 kHz acoustic positioning system installed on the receiver monitoring ship with transponders on the two receiving arrays.

The transmission run was structured with separate 40 km legs such that the receiving arrays were oriented cross, up and downslope with respect to the source ship radial tracks. The source ship speed (8 kts) and rate of source expenditure were designed to achieve a spatial sampling of the propagation field with a 1 km interval. During the transmission run the signal repeater ship ran parallel legs with respect to the source ship and transmitted continuous tones at 56, 129 and 314 Hz.

Reverberation runs were arranged to provide a near monostatic geometry (source-to-receiver separation of 1 km) and bistatic geometries with cross-slope source-to-receiver separations of 10 to 40 km in 10 km increments. The signal repeater was positioned due

north of the receiving arrays at a range of 25 km. To insure statistical stability of derived scattering strength estimates, measurements with 6 explosive sources were made for each of the bistatic reverberation geometries and for the monostatic geometry 12 sources were used [2].

Together with the acoustic measurements described above, supporting environmental data were gathered during the test. A side scan sonar sea floor topography and 3.5 kHz sub-bottom profile survey of the bottom at the receive array site was conducted by the receiver monitoring ship prior to deployment of the arrays. The side scan sonar was also used to image the bottomed horizontal line array at the completion of the test. The signal repeater ship, under the direction of Naval Research Laboratory, Stennis Space Center (NRL-SSC) personnel, collected Shipek grab samples of the ocean bottom sediment and deployed a Tropical Oceanographic Global Atmospheric (TOGA) buoy which recorded sea surface temperature, air temperature, barometric pressure, wind speed and wind direction and transmitted the recorded data via an Argos satellite relay to a central station daily. Conductivity-Temperature-Depth (CTD) casts were conducted before and after the test and twice during ACT I by the receiver monitoring ship and by the signal repeater ship; Expendable Bathythermograph (XBT) deployments were performed every 6 to 8 hours by each of the three participating ships.

## 3. Environmental Description

The ACT I site bathymetry contours (Figure 1) are directed northwest-southeast, with shoaling to the northeast. Water depths in the test area varied from 80 m to 450 m and at the array site was 182 m. For the most part the geoacoustic properties of the bottom were homogeneous over the test site and the oceanographic characteristics homogeneous over the area and stationary during the test period.

Similarly, meteorological conditions did not change over the period covered by the data reported here. Throughout the measurement period discussed in this paper, the sea surface was glassy-to-lightly rippled, consistent with a Beaufort wind force 0-1. Winds ranged from flat calm to 2 m/sec during the period of these measurements.

### *3.1. Oceanographic Characteristics*

The ocean in the ACT I area is most strongly influenced by local Gulf of Mexico surface water and Carribbean Sea Intermediate water, the latter being characterized by subsurface salinity maxima clearly seen in the CTD casts from the signal repeater ship. The salinity maxima coincided with the depth interval of maximum temperature variability (80-180 m depths). However, there was little change in the mixed layer depths over the ACT I period; rather the variability seen below 80 m is indicative of warmer subsurface water in the northeastern section of the test area as compared with the cooler subsurface waters found in the offshore regions. The XBT casts were interpolated and merged with salinity from the nearest CTD cast. Sound speeds were computed from Wilson's equation and are shown grouped for the entire test site in Figure 3. The sound speed is observed to vary (systematically) by as much as 10 m/sec between 125 and 150 m depth.

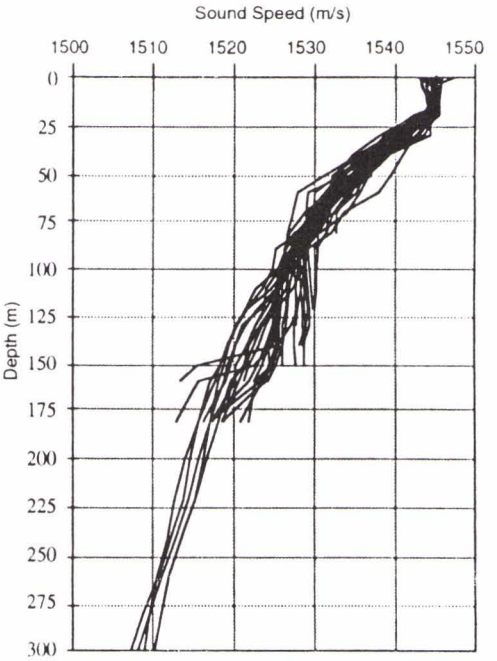


Figure 3. Composite of sound speed profiles measured over test area.
(Data from NRL-SSC)

On the West Florida Shelf at the test site area the interaction of continental shelf water and the Loop Current can at times create complex eddy and frontal systems often manifested by alternating cold shelf and warm Loop Current intrusions. However, measurements of current made at the array site indicated only small currents of 5-10 cm/sec at midwater depth. Thus, during ACT I the Loop Current was not in evidence nor was there evidence of other dynamic processes that could precipitate significant variability in the sound speed field.

*3.2. Geoacoustic Characteristics*

The limited 3.5 kHz sub-bottom profile records obtained on the receiver monitoring and signal repeater ships indicate a sharp reflection from the water-sediment interface with sub-bottom penetration to approximately 5 m and little indication of stratification to that penetration depth. Absence of stratification in the top few meters below the bottom does not obviate stratification at lower depths and indeed acoustic pulse arrival data from the test indicate the existence of sub-bottom structure (see Section 4.1).

The sediment grab samples gathered on the signal repeater ship confirmed that the surficial sediment properties over the test site were generally homogeneous, with all 7 samples consisting of similar greenish-gray sandy material. Although noncohesive grab samples typically "wash out" during retrieval, portions of the samples remained firm and intact suggesting a significant clay content. Initial sediment grain size analysis classified these

samples as sand-silt-clay [3], as indicated in Figure 4. For this sediment classification, values of bottom parameters taken from Hamilton [4] were averaged to obtain the following surficial sediment properties: compressional sound speed ratio = 1.061, sediment density = 1.701 g/cm$^3$, and attenuation coefficient = 0.10 dB/m kHz. An estimate of acoustic losses using these bottom properties indicates bottom reflection losses of less than 1 dB out to grazing angles of about 20°, with a steep increase in bottom loss for higher grazing angles.

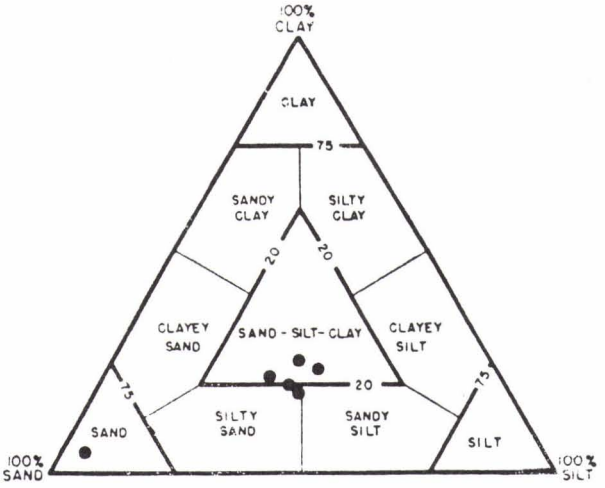


Figure 4. Shepard sediment composition chart showing composition of samples from test bottom sites. (Data from NRL-SSC)

## 4. Acoustic Transmission Measurements

From the perspective of active sonar performance, acoustic transmission characteristics of concern are: transmission loss as a function of range, depth and frequency (to affirm or reject the assumption of independence of reverberation limited performance on transmission loss and, of course, to ascertain that there is sufficient signal to see the target above ambient noise); spatial coherence of transmitted signals as a function of range and frequency (to establish what effective signal array gain can be achieved); signal pulse spreading as a function of range and frequency (to ascertain the importance of temporal dispersion in determining active bottom reverberation area). In addition to the factors noted, the temporal multipath structure and vertical angle of arrival structure of small impulsive signals used in the test will also be described. These latter features highlight significant properties of the acoustic channel and provide further information on transmission mechanisms.

### *4.1. Pulse Propagation*

The signal arrival structure from a small (1 gm of net explosive weight) explosive source detonated at mid-water depth and received at a range of 13 km over the band 25 Hz to 1 kHz on a phone at the bottom is shown in Figure 5. In the received signal a distinct sequence of arrivals can be seen with each member corresponding to n bottom bounce and n or n+1 surface reflected paths (the sources used here were sufficiently small that the

bubble pulse was not resolved in the arrival structure). The steepest paths observed correspond to bottom grazing angles of 30° or more, somewhat in excess of the expected critical angle near 20° for the sand-silt-clay sediment at the test site. Indeed, there is no evidence in the arrival structure of a sharp cutoff in transmission at a well defined grazing angle at the bottom.

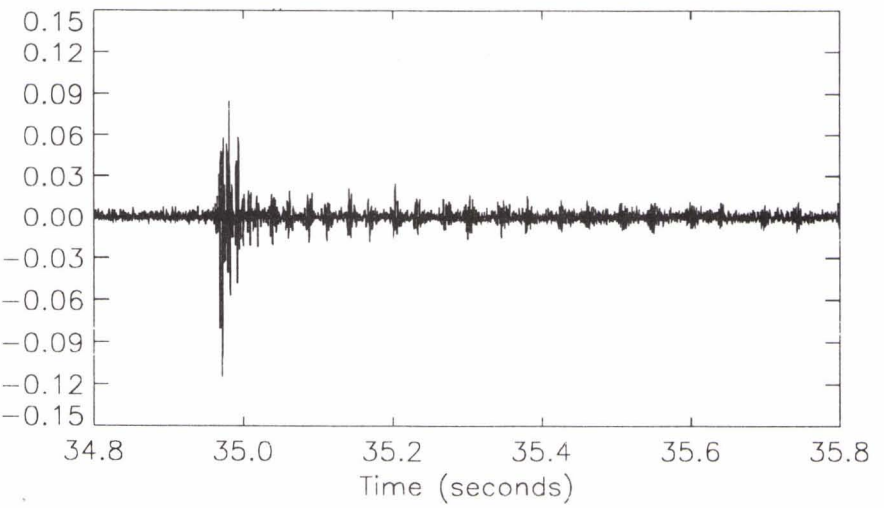


Figure 5. Pulse arrival structure for source at 90 m depth and receiver on bottom (182 m) with 13 km separation.

Insight into this result can be gotten from Figure 6, which shows stacked time traces of the initial signals received on the phones of the vertical line array (with phone 1 at 102 m above the bottom and phone 25 at 4.5 m above the bottom) from a source at a range of 359 m. In Figure 6 the initial arrival at each phone is the direct path signal and the phase inverted arrival on phones 1-15 at the upper right of the figure is the surface reflected signal. A weak arrival is observed on all phones, the extrapolation of whose leading edge trace would intercept the extrapolation of the trace of the direct arrival at the bottom, 4.5 m below phone 25. A closely trailing arrival, which is stronger than the bottom reflected arrival, represents a signal which has reflected from a layer at a depth approximately 8 m below the surficial bottom, the layer depth again determined by extrapolation of the leading edge trace. The data in Figure 6 indicate the existence of a fast sub-bottom layer at about 8 m below the water-sediment interface that strongly reflects bottom penetrating signals (i.e., signals having bottom grazing angles greater than the nominal critical angle of about 20°).

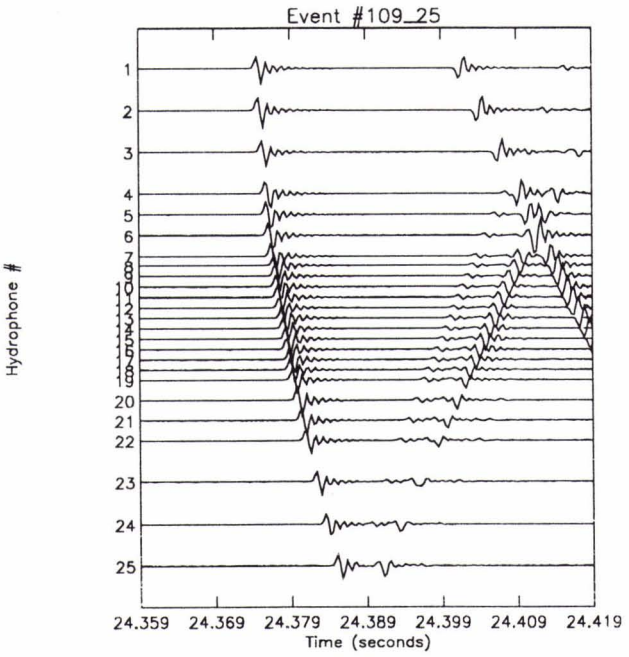


Figure 6. Stacked time traces of the initial arrivals at the vertical array elements for a source at 359 m range.

*4.2. Pulse Spreading*

Pulse spreading influences sonar performance by reducing the received signal-to-interference ratio from what could be realized if all the target echo energy were received within a time interval less than the transmitted pulse resolution. A practical value useful for sonar performance was determined from the ratio of post-rectification integrated echo signals to integrated reverberation as a function of the integration time. The effective pulse time spread was evaluated as the largest integration time for which the signal-to-interference did not begin to monotonically diminish.

Two-way pulse spreading was determined for the signal repeater at a range of 26 km upslope for the three octave processing bands from 50-400 Hz. Time spreads obtained in this fashion were averaged over 4 events and the results are shown in Figure 7. The frequency dependence of the measured time spreads may have been influenced by the signal-to-background ratios of the received pulses, which averaged 13 dB for the 50-100 Hz band, 8 dB for the 100-200 Hz band and 8 dB for the 200-400 Hz band. Separately, the effect of pulse integration time on the determination of one-way transmission loss was also examined. It was found that more spreading occured upslope than down by a factor of 2-3, implying that the upslope propagation path dominated the two-way time spread values.

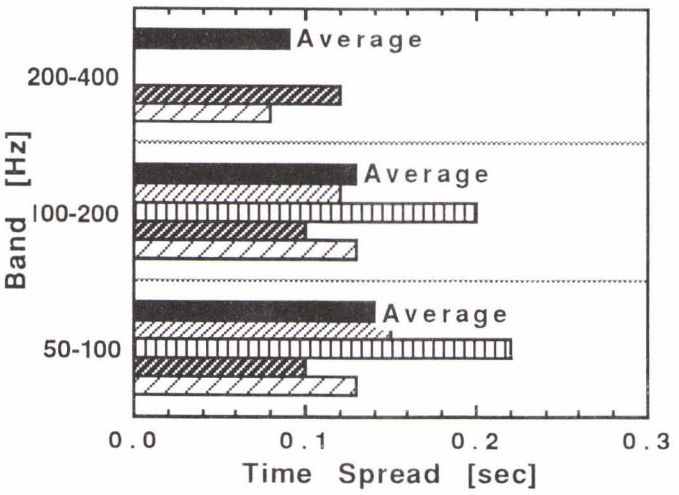


Figure 7. Two-way pulse spreading for 4 shots to and from a signal repeater at 26 km.

*4.3. Signal Coherence*

The spatial coherence of transmitted signals is a measure of the signal similarity at spatially separated points and is evaluated as the peak of the normalized cross correlation. The horizontal coherence transverse to the direction of propagation of the explosive signals received at different phones on the horizontal array was computed for source-to-array ranges of 14 and 30 km. Measured transverse coherence as a function of reduced separation $kd$, where $k = 2\pi/\lambda$, with $\lambda$ = acoustic wavelength and $d$ = spatial separation, is shown in Figure 8 for three sources at a range to the receiving horizontal line array of 14 km. From the data in Figure 8 the coherence is observed to exceed 85-90% for spatial separations of 36 wavelengths. Similar results were obtained at a range of 30 km.

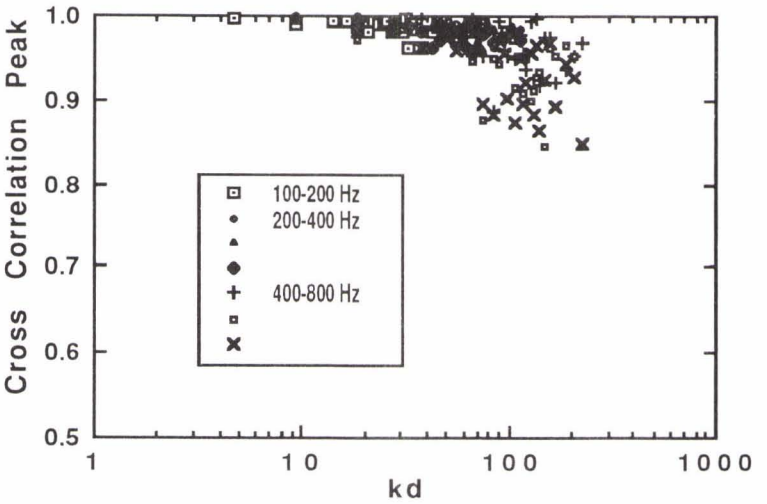


Figure 8. Horizontal transverse coherence for three sources at a range of 14 km.

Another effect that can cause a degradation in signal gain at a sonar beamformer output is jitter of the signal arrival time at the sensor. The delays of the peaks of the cross correlations between all the phones and an end phone from a shot received on the horizontal line array were measured. The array element positions were computed from the measured correlation peak delays under the assumption of conserved interelement separation. These computed array element positions are shown in Figure 9 for three shots at 14 km source range. The slight curvature of the array apparent in Figure 9 is completely consistent with a 1.5 m bow in the array determined using the side scan sonar. Jitter in the computed element positions was determined to be no larger than sampling noise error associated with the 3.3 kHz sampling rate used in the Seacal units.

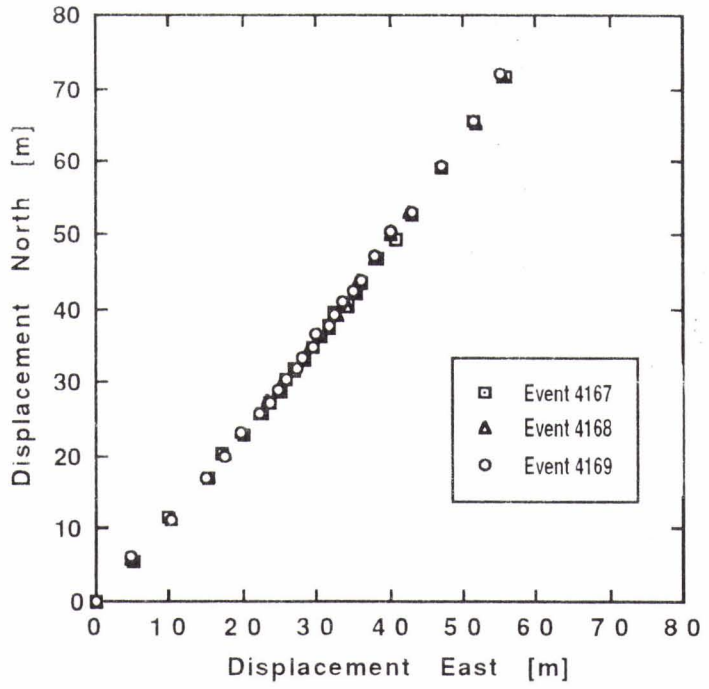


Figure 9. Horizontal line array element locations reconstructed from the correlation peak delays for each element relative to an end element.

The high observed coherence and absence of arrival time perturbations imply that nearly ideal signal gain performance can be expected for this site. To verify this signal array gain degradation was directly computed for a beamformer that removed the effect of array curvature; signal array gain degradation was found to be about 1 dB for a 36 wavelength array in the 400-800 Hz band for both 14 km and 30 km source ranges.

*4.4. Transmission Loss*

Transmission loss in shallow water is known to be more favorable than free field propagation (spherical spreading) at short to intermediate ranges (because of the waveguide effect of surface and bottom) and to be worse at longer ranges (because of boundary losses). Unfortunately the great variability of shallow water propagation obviates

quantitative insight into expected transmission loss for many situations and direct measurements must be invoked. ACT I transmission loss data have been analyzed in octave frequncy bands as functions of range and depth and also as a function of frequency at several ranges. In determining transmission loss for the measurements, source level and energy spectra of the sources from a previously conducted calibration test were used; source data were recorded on a monitoring phone suspended from the source ship during the transmission measurements but these data have not yet been factored into results reported here.

The range dependence of transmission loss for mid-depth and bottom receivers as measured during the test in the 4 octaves from 50-800 Hz is shown in Figure 10. Except for the 400-800 Hz band upslope transmission, transmission losses both upslope and downslope are better than spherical spreading to 30 km. Beyond this range the slope of transmission loss with range worsens, especially for upslope propagation. This is indicated in more detail in Figure 11 which show transmission loss versus frequency at three ranges, 9, 18.5 and 28 km. These data can be summarized as follows: transmission

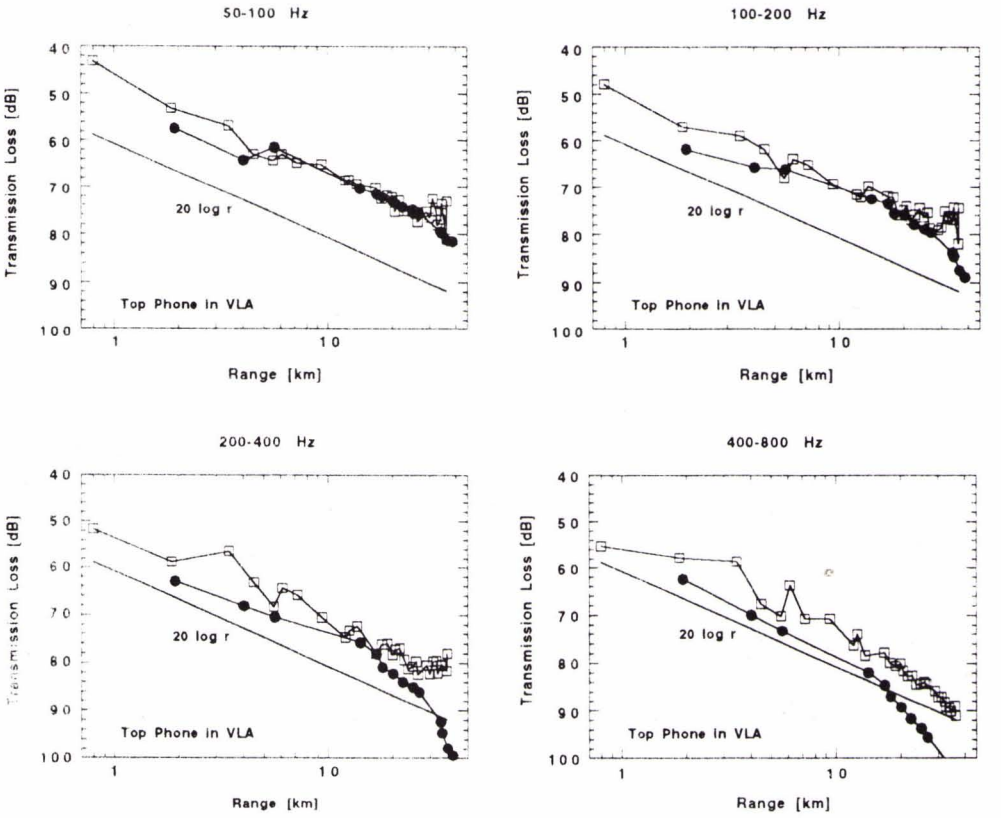


Figure 10. Comparison of transmission loss vs range for upslope (solid circles) and downslope (open squares) propagation in the 4 one-octave bands from 50-800 Hz for source and receiver at 90 m depth.

loss upslope, initially better than spherical spreading below 1 kHz, is worse than spherical spreading beyond 18.5 km (10 nmi) above 400 Hz; transmission downslope, initially better than spherical spreading below 1 kHz, is worse than spherical spreading beyond 18.5 km above 600 Hz.

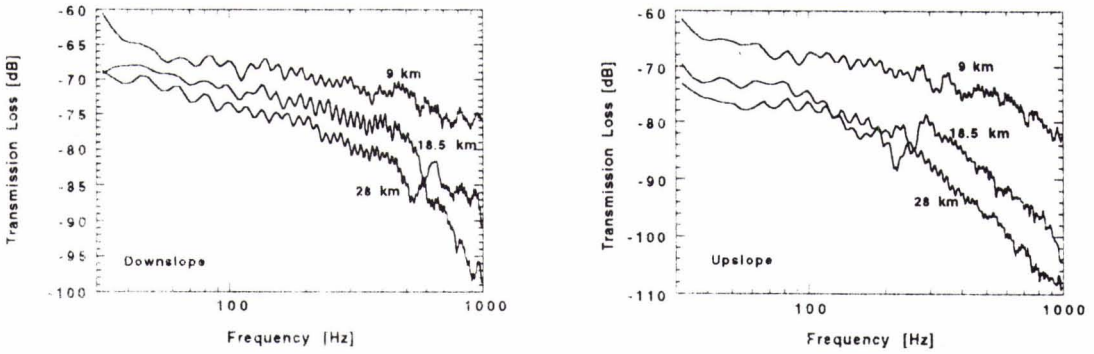


Figure 11. Variation of transmission loss with frequency at ranges of 9, 18.5 and 28 km in the one-octave bands from 50-800 Hz.

The depth dependence of transmission loss is shown in Figure 12 where transmission losses at 9, 18.5 and 28 km are plotted vs vertical line array hydrophone height off the bottom for upslope and downslope propagation respectively. The variability of transmission loss with depth is about ±2.5 dB, substantially independent of range, slope orientation and frequency. This variation with depth is not significantly different from the variation about a smoothed or mean transmission loss vs range as shown in Figure 10.

These considerations suggest that the assumption that sonar performance in shallow water under bottom reverberation limited conditions is independent of transmission loss is a reasonable assumption for performance estimates using the sonar equation (i.e., estimates based upon mean levels of signal-to-interference).

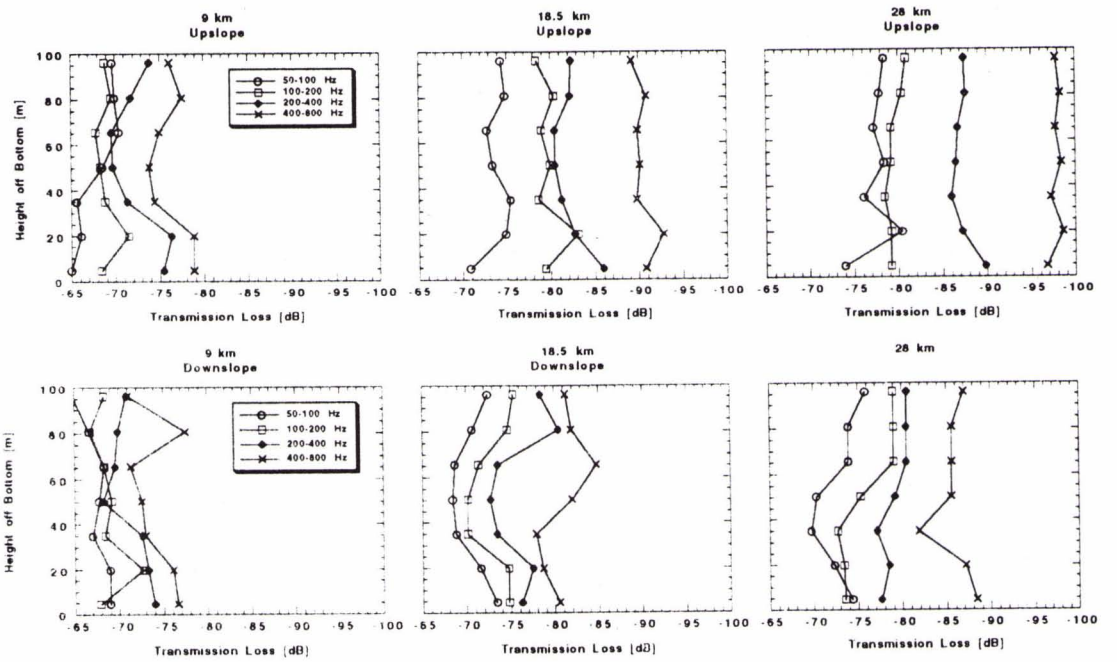


Figure 12. Variation of transmission loss with depth at ranges of 9, 18.5 and 28 km for source and receiver at 90 m depth.

## 5. Reverberation Measurements

Determination of low frequency bottom scattering strength in shallow water is more complicated than in deep water because it is not possible to design single path scattering geometries for shallow water. Thus scattering strength determinations for the test area involve inferring bottom scattering strength from measurements of reverberation. The low sea states and downward refracting propagation conditions that existed during the test insured that bottom reverberation and not surface reverberation was the dominant boundary scattered component. Besides bottom scattering strength the azimuthal directionality of the reverberation field will also be described because of the insight that can be gained on the effect on reverberation of bottom slope.

### *5.1 Monostatic Bottom Scattering Strength*

For the test and environmental conditions in ACT I, it was estimated that fathometer bottom returns at the receiver would decay below the reverberation level in about 3.5-4 sec (2.6-3

km), permitting reliable estimates of total scattering strength (that is, integrated over incident and scattering angles) to be made after the short dominance of fathometer echoes.

The scattering strength $SS$ [dB] is determined as [5]

$$SS = 10 \log(I_S / I_i), \tag{1}$$

where $I_i$ is the incident intensity at the bottom (assumed to be plane wave sound) and $I_S$ is the intensity of sound scattered from a unit area of bottom, measured at a large distance from the bottom and referred back to unit distance from the bottom.

It can then be shown that the bottom scattering strength is determined from [6]

$$SS = RPL - ESL + 2TL - 10 \log r - 10 \log(\pi c), \tag{2}$$

where $RPL$ = reverberation power level in band [dB//μPa], $ESL$ = energy source level in band [dB//μPa sec @ 1m], $TL$ = transmission loss one-way [dB//m$^2$], $r$ = range to reverberant patch [m], $c$ = sound speed at reverberant patch [m/sec]. Bottom scattering strength determinations were computed using the measured reverberation spectra, the previously determined source energy spectra and levels, and transmission losses, estimated as described previously, averaged for up and downslope propagation (it should be noted that, because the same type of sources were used to make transmission loss and reverberation measurements, the scattering strength determinations are self calibrated). Scattering strength determinations in the 4 octave bands from 50-800 Hz were determined to be independent of range beyond 6-8 km (8-10 sec)

Estimated asymptotic bottom scattering strength versus frequency for the ACT I site is given in Figure 13 and compared with earlier results of Urick [7] obtained at a Gulf of Mexico location about 100 mi southeast of the ACT I site; at Urick's site the bottom was clayey silt with numerous shell fragments. The two independent determinations of bottom scattering strength are comparable at low frequencies but differ by about 3 dB at the upper end of the band. In Figure 13 the estimates of scattering strength from the Gulf of Mexico are also compared with determinations of scattering strength reported by Thiele and Tielburger [8] for sand bottoms from a number of North Sea and Baltic Sea locations. Above 100-200 Hz the ACT I scattering strengths are at the high end of values obtained from the North Sea and Baltic Sea. But the most striking difference is that the Thiele and Tielburger data show a distinct minimum in the scattering strength at 100-200 Hz with a sharp rise at low frequency whereas the ACT I data are monotonic and increasing with frequency above the lowest measurement frequency of 50 Hz. Thiele and Tielburger explain the increase in scattering strength at low frequency as being caused by structure within the bottom scattering the deeper bottom penetrating low frequency sound. Correspondingly, the absence of an increase in scattering strength at low frequency in the Gulf of Mexico results may indicate an absence of scattering structure within the upper sediment.

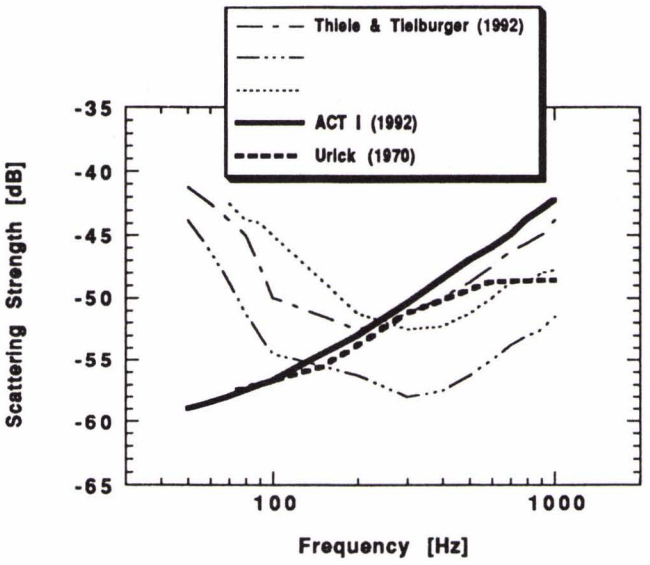


Figure 13. Comparison of shallow water sand bottom scattering strength measurements as a function of frequency.

*5.2 Azimuthal Dependence*

Figure 14 depicts the azimuthal dependence of monostatic reverberation obtained from the horizontal array beam outputs. The levels have been adjusted only to remove the effect of beamwidth so that the plot depicts constant angular resolution. It is clear from Figure 14 that there is increased reverberation in the upslope direction as compared with the cross-slope direction and an indication of slightly reduced reverberation in the downslope direction. These effects are expected from basic considerations. Also noted in the plot are bands of increased reverberation in the upslope direction that ray traces indicate are associated with propagation caustics at the bottom.

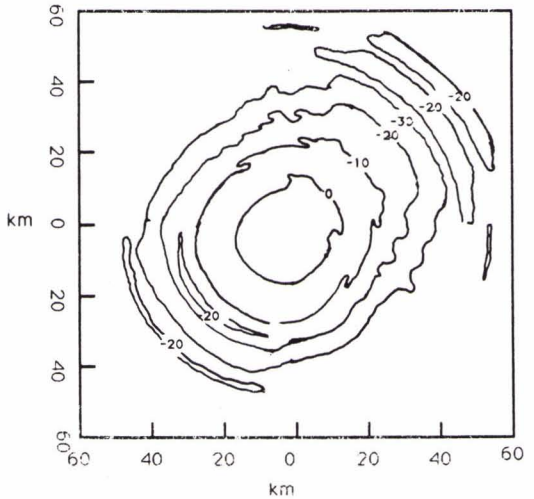


Figure 14. Azimuthal variation of relative reverberation level. The upslope direction is toward the upper right corner of the plot.

## 6. Conclusion

ACT I has provided measurements of the key sonar parameters for a specific shallow water site. Environmentally the site was acoustically adverse (strong downward refracting sound speed profile) but homogeneous and stable over the test period, with a high impedance, sand-silt-clay bottom that sloped slightly. Transmission loss tended to be high with propagation becoming worse than free field at 20 km for frequencies above the mid-hundreds of Hertz. Multipath pulse spreading was 100-150 msec. Transverse spatial coherence was high, exceeding 85-90% for up to 36 wavelength sensor separations at all ranges to 30 km. Bottom scattering strengths were monotonically increasing with frequency, ranging in value from about – 57 dB at 40 Hz to – 45 dB at 1 kHz.

The results obtained in this test are in general agreement with various reported results on separate aspects of downward refracted transmission, signal coherence and reverberation in shallow water areas having fast bottoms and thick sediment layers. The results obtained in ACT I encourage the conclusion that the relevant parameters have been determined to permit intelligent sonar design and performance estimation to be conducted for this and similar shallow water regions.

## Acknowledgements

The authors are indebted to Jim Matthews and Bruce Gomes of the Naval Research Laboratory, Stennis Space Center, for their invaluable contribution in conducting the oceanographic, bottom geoacoustic and mereorological measurements and analyses for the work reported here. We also wish to thank the ships' crews and staff from Survey Boats Incorporated and from John E. Chance Associates for their unstinting cooperation in supporting ACT I. Finally, we want thank Bill Carey of DARPA for his technical guidance and vision which significantly aided the planning and conduct of ACT I.

## References

[1] Tattersall, J.M., King, P., Mingrone, J and Herstein, P. The Aoustic Transient Recording Buoy (ATRB): System description and initial measurement results. *IEEE Journal of Oceanic Engineering*, **17**, 1992: 227-238.

[2] Barrick, D.E., Accuracy of parameter extraction from sample-averaged sea-echo Doppler spectra. *IEEE Trans. Antennas Propagat.* **AP-28**, 1980: 1-10.

[3] Matthews, J., Preliminary geoacoustics for ACT I area. Private Communication

[4] Hamilton, E.L. and Bachman, R.T., Sound velocity and related properties of marine sediments. *J. Acoust. Soc. Am.*, **72**, 1982: 1891-1904.

[5] Urick, R.J., Principles of Underwater Sound. New York, NY, McGraw-Hill, 1975.

[6] Urick, R.J., Generalized form of the sonar equations. *J. Acoust. Soc. Am.*, **34**, 1962: 547-550.

## References *(Cont'd)*

[7] Urick, R.J., Reverberation-derived scattering strength of the shallow sea bed. *J. Acoust. Soc. Am.*, **48**, 1970: 392-397.

[8] Thiele, R. and Tielburger, D., Broadband omnidirectional reverberation measurements in shallow water with explosives. *In*: Ocean Reverberation Symposium. La Spezia, Italy, SACLANT Undersea Research Centre, 25-29 May 1992.